International Society for Rock Mechanics and Rock Engineering
Norwegian Group for Rock Mechanics

ISRM International Symposium
Eurock 2025 – Expanding the Underground Space
Trondheim, Norway, 16-20 June
ISBN 978-82-8208-079-8

Tensile-shear stress induced crack initiation in granite specimens loaded in compression

L. Jacobsson
RISE Research Institutes of Sweden, Borås, Sweden
lars.jacobsson@ri.se (email of corresponding author)

Abstract

A novel type of experiment was developed where the crack initiation of medium-grained granite was studied in detail. Flat specimens with a discontinuous width were loaded in compression and the strain was measured by strain gauges on the sides and displacements by Digital Image Correlation on the flat surface. The cracking process was studied using acoustic emission monitoring. The specimen geometry yields a stress concentration with a mixed tensile and shear stress state. Specimens with three different discontinuity sizes were tested to study the discontinuity size in relation to the grain size. The results show that the discontinuity size affects both when crack initiation occurs and the crack propagation path. The crack patterns were assessed using images taken on the specimen during loading.

Keywords

Crack initiation, brittle rock, acoustic emission, digital image correlation

ISRM

NBG

1 Introduction

There is an interest to understand the conditions for initiation and propagation of cracks in rock material close to a surface or around defects. Examples of applications range from surface spalling at underground openings in various tunnels, large deposition holes for nuclear waste, in smaller boreholes or at loaded pillars. There is a hypothesis and evidence that tensile cracking, mode I, is the fundamental fracture mode at surface spalling in hard rock at low confinement stress.

Failure of brittle crystalline rock at compression were studied by Horii & Nemat-Nasser (1986). They used the wing crack theory to explain how compressive loading results in tensile failure. Germanovich & Dyskin (2000) studied failures around underground openings and found similar conclusions.

The novel experiments described in this paper are used to investigate the crack initiation and propagation of cracks in granite where a mixed tensile and shear stress state are obtained at the vicinity of an inward directed corner in planar specimens. The idea is to study the competition between tensile versus shear induced cracking in relation to the microstructure size, in this case the grain size.

2 Experiments

2.1 Specimens

The specimens are made of a medium-grained granite from the Flivik quarry in Sweden. The specimens are taken from the same host block as the specimens described in Jacobsson & Lindqvist (2018). The specimens are made from six rectangular plates that are slices next to each other obtained from a longer rectangular block. A cut-in was made on one side of the specimens resulting in a narrower width on a part of the side and yielding an inward corner. Six specimens with three different cut-in depths were manufactured. A sketch of the specimen design is shown in Fig. 1 and dimensions are found in Table 1. The specimens were carefully grinded with high precision yielding smooth and planar surfaces which all were parallel, respectively perpendicular, to each other. The cut-ins were made by carefully milling the specimens. The radii of the inward corners were measured using an optical profile projector. An example is shown in Fig. 2. The radii, *r*, were in the range of 0.1-0.7 mm.

The granite has an isotropic material structure. Quarried granite is known to have oriented microcracks, e.g. Nadan & Engelder (2009), yielding anisotropic mechanical behaviour. The specimens were manufactured such that the rift plane is parallel to the width of the specimens.

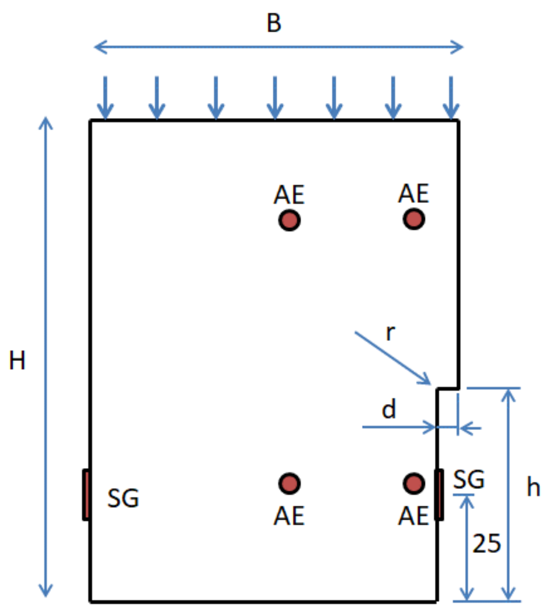

Fig. 1 Schematic illustration of the specimen geometry including sensors for acoustic emission (AE) measurements and strain gauges (SG).

Table 1 Specimen dimensions with definitions in Figure 1. The thickness is denoted *t*. All dimensions are given in mm.

Specimen	B	H	t	h	d
A1	90.37	120.13	10.45	50.15	2.05
A2	90.38	120.11	10.45	50.21	2.07
B1	90.37	120.09	10.45	50.30	4.06
B2	90.37	120.12	10.45	50.29	4.06
C1	90.37	120.11	10.46	50.30	8.05
C2	90.37	120.10	10.46	50.25	8.04

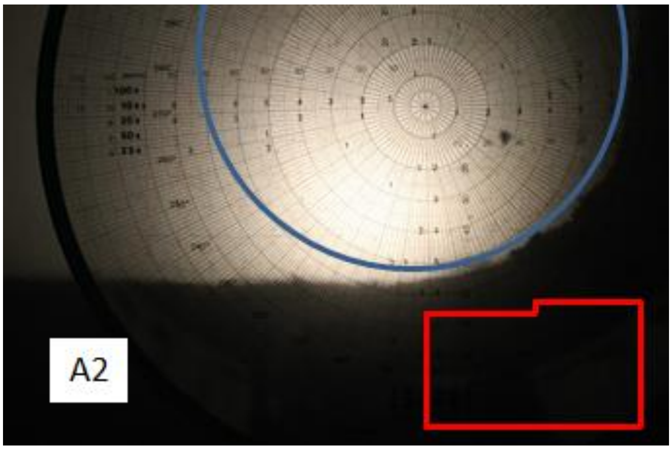

Fig. 2 Notch radius of specimen A2 measured using a profile projector at 100x magnification. The blue circle corresponds to a radius of 0.7 mm. A scale is shown in the background. The red image illustrates the specimen orientation.

2.2 Test setup

The specimens are loaded in axial compression where the specimens are compressed between planar loading platens of hardened steel. There is a spherical bearing mounted on top of the upper loading platen allowing the platen to align to the specimen. This yields an even loading on the compressed surfaces of the specimens. The specimens were loaded at constant displacement rate of 0.12 mm/min up to when severe cracking occurred and then stopped. A picture of the test set-up from the laboratory is shown in Fig. 3.

The specimens were instrumented with two strain gauges, with a 12.7 mm gauge length, from Micro Measurements, at the lower parts of the sides. Four acoustic emission (AE) sensors were placed on each specimen to make it possible to monitor crack noise emission levels and localisation of crack events. Micro30 sensors were used for the AE measurements. The AE sensors, acquisition system and software were from Physical Acoustics Corporation (PAC). The AE sensors were placed at the coordinates [*x*, *y*] = [5, 50], [45, 50], [5, -30] and [45, -30]. Fig. 4 shows the coordinate system definition. The coordinate values are given in millimetres.

The deformation field was measured using digital image correlation (DIC) on one face of the plate. The DIC system Aramis 12 M from GOM GmbH was used for the measurements. The measuring area was c 100 mm × 80 mm.

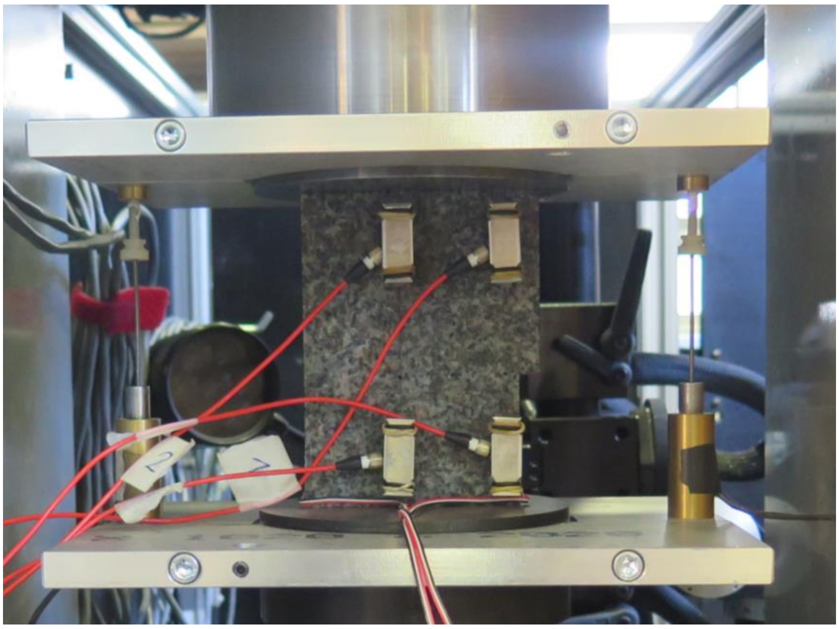

Fig. 3 Specimen placed between loading platens. The acoustic emission sensors are seen on the front side. The DIC system can partially be seen behind the specimen monitoring the rear side.

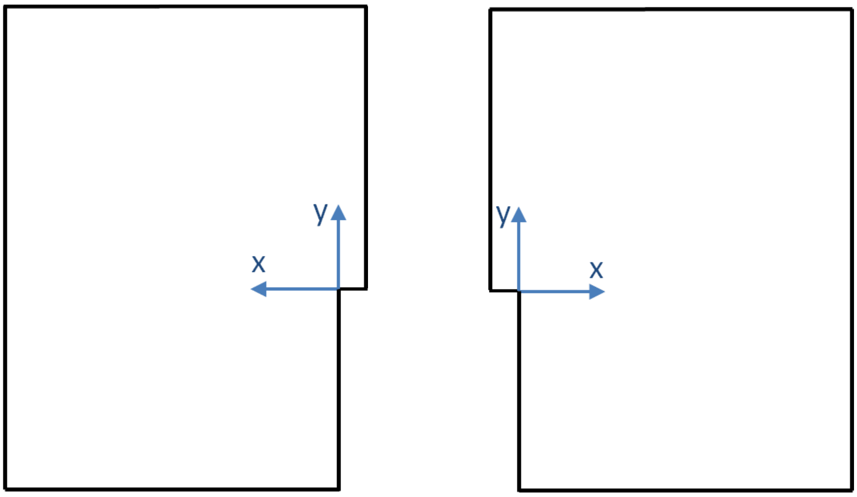

Fig. 4 Definition of coordinate system for localization analysis of acoustic emission signals. Left: Front side view; Right: Rear side view.

3 Results

3.1 Experiments

The specimens were tested in the order C1, C2, B1, B2, A1 and A2. The specimens were loaded until a fracture was fully developed at the corner side and a piece of the specimen was detached. This worked well for the C- and B-specimens. When specimen A1 was tested, the loading continued until a complete specimen failure occurred. The test of specimen A2 was therefore prematurely aborted before a specimen failure occurred. No fully developed fracture, yielding a whole fragment detachment from the specimen at the corner area, was obtained for specimen A1 and A2. Pictures of specimen B1, B2, C1 and C2 taken after the testing are shown in Figs. 5 and 6. Similar pictures of the A-specimens are omitted since no crack in the corner is visible. The images of the B-specimens show that the fracture was going from the inward corner and going vertically and deflecting out to the side without going all the way to the top of the specimen. The fractures on the C-specimens goes from the corner area all the way to the top.

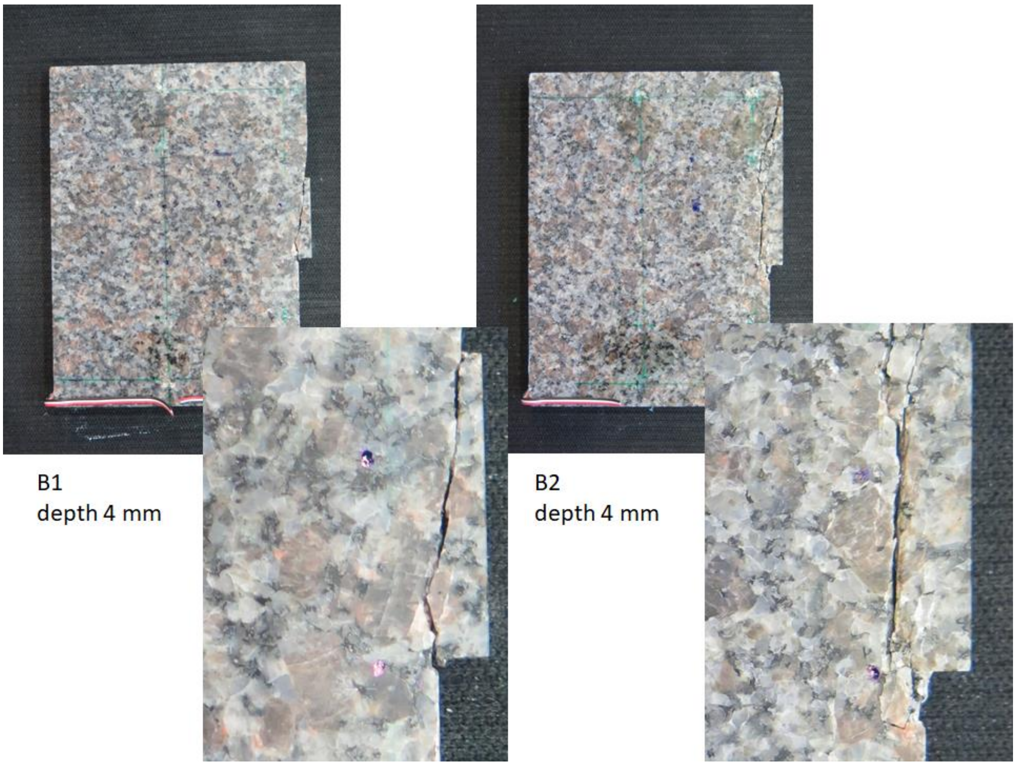

Fig. 5 Specimens B1 and B2 photographed after testing.

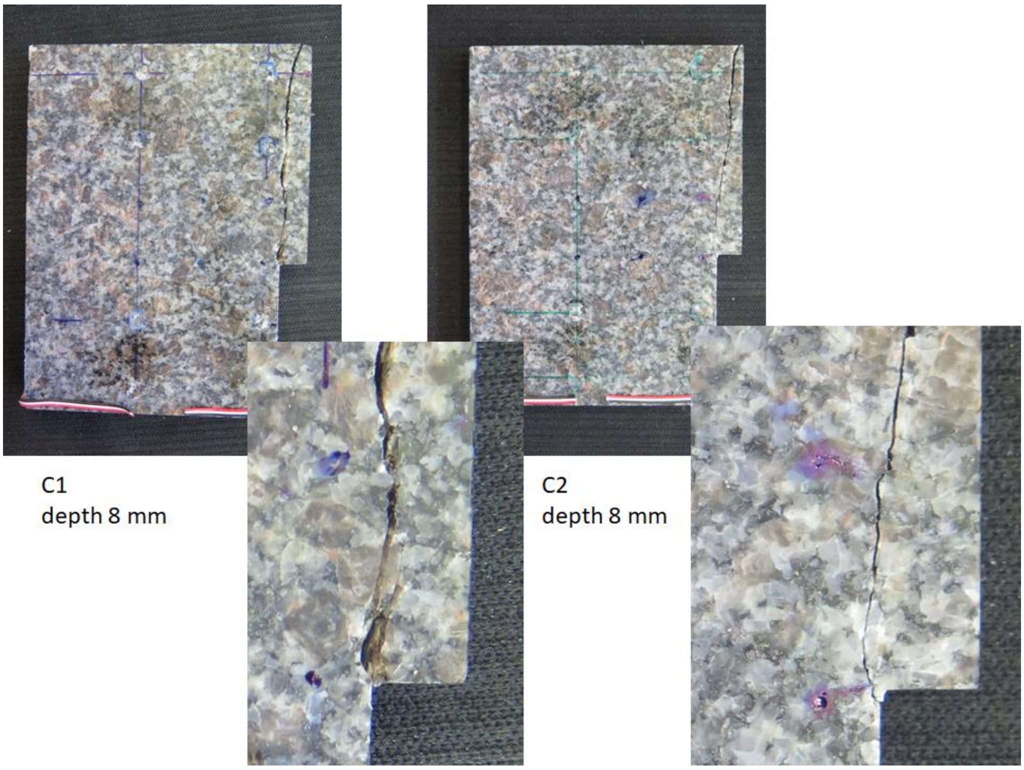

Fig. 6 Specimens C1 and C2 photographed after testing.

3.2 Results from AE measurements

An amplitude-based hit trigger criterion was used with a threshold value of 50 dB. The program AEwin from PAC was used for the hit localization analysis. The wave propagation velocity 3750 m/s was used in the analysis. The value was determined by means of the data generated during the automatic sensor test. The accumulated acoustic events for a calculated source amplitude larger than 60 dB, localized within the rectangular area x = [-10, 20] mm and y = [-10, 30] mm containing the corner region, were determined. A diagram showing the accumulated events versus the applied force is shown in Fig. 7. Events started to be recorded above a force of c 62 kN. The accumulation of events for the B- and C-specimens display a sudden increase of the acoustic events that can be related to crack propagation. The A-specimens do not show any sudden increase as for the B- and C-specimens, except for possibly at a very late stages of the loading.

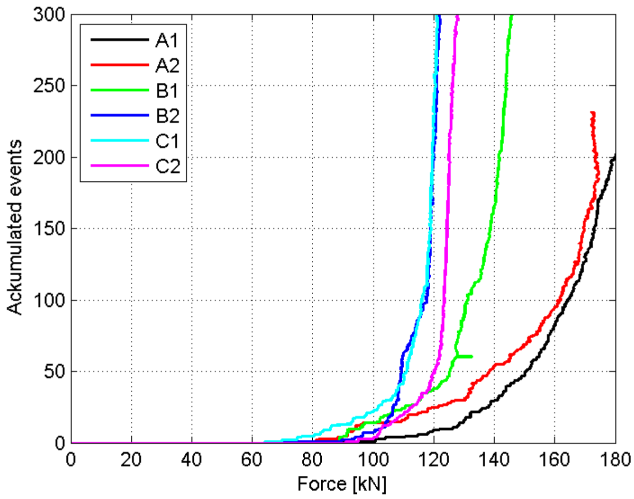

Fig. 7 Accumulated acoustic events localized to the area of the specimen with the inward-directed corner.

3.3 Crack observations from images on the specimens

The cracking process can be seen from images taken on the specimens for the DIC analysis. The cracking process is qualitatively described by schematically showing the crack patterns and applied force at the initiation. The results from the assessment of crack patterns are shown in Figs. 8–10. It shall be noted that the assessments are subjective and preliminary. The crack initiation is closer to the corner at the A-specimens and tend to be farther away from the corner with increasing cut-in size, although the variation between the specimens is large.

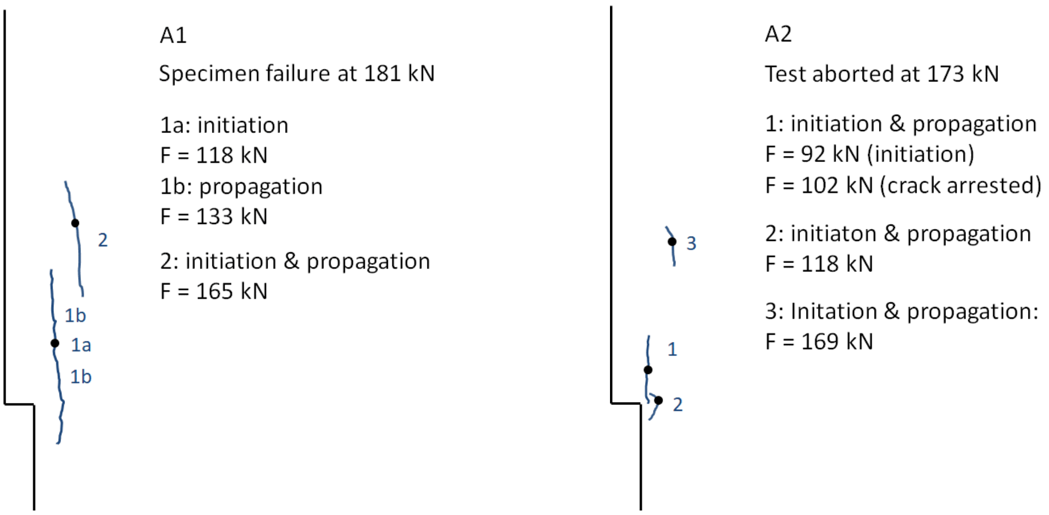

Fig. 8 Observed cracks from images in specimens A1 and A2. Black dot marks the initiation location.

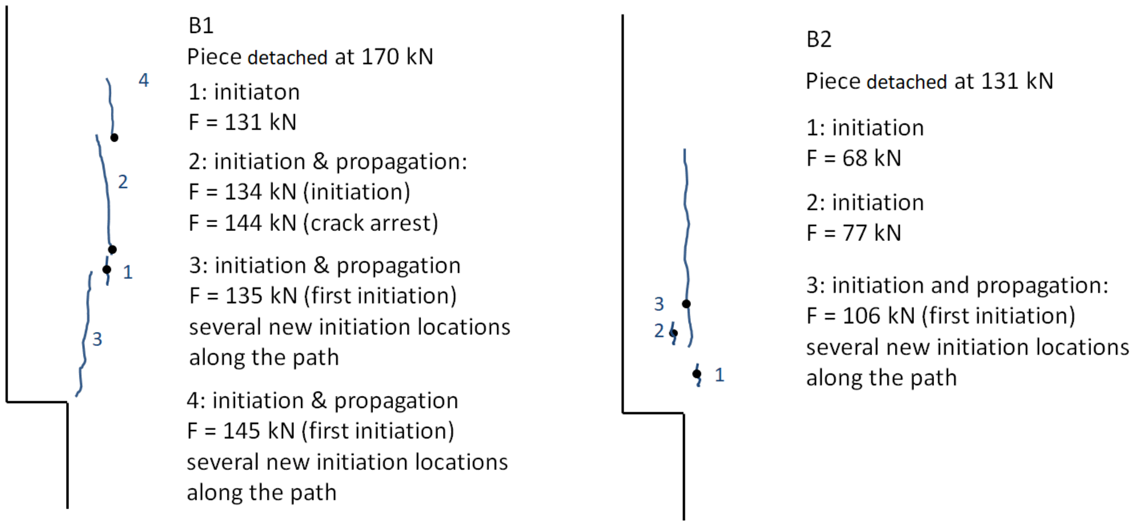

Fig. 9 Observed cracks from images in specimens B1 and B2. Black dot marks the initiation location.

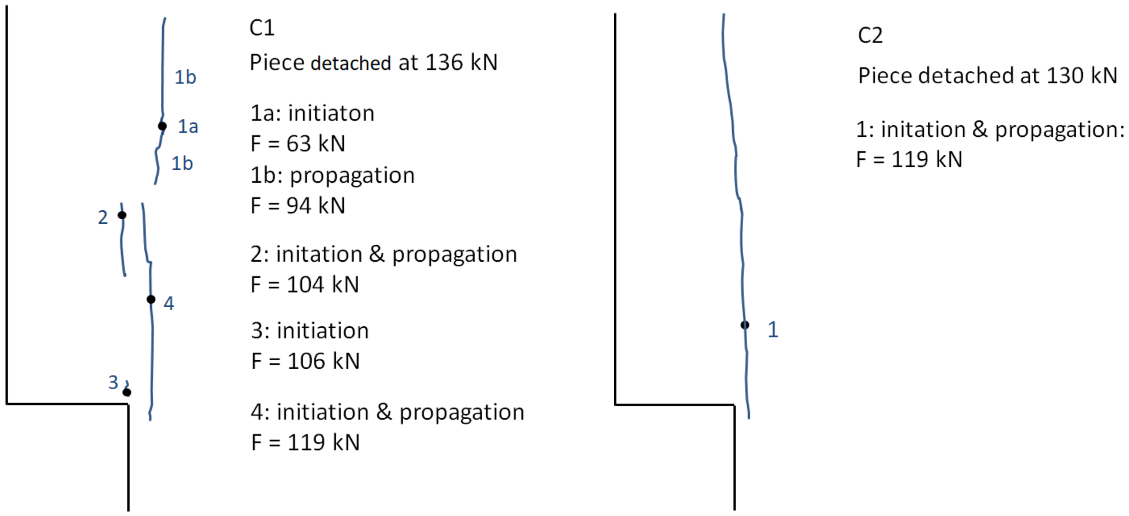

Fig. 10 Observed cracks from images in specimens C1 and C2. Black dot marks the initiation location.

3.4 Results from the Digital Image Correlation analysis

Results from DIC measurements of the lateral displacement (x-direction) is shown in Fig. 11 for specimen C2 at three loading stages as an example. The image for the stage with the lowest load shows that some localized deformation begins to take place above the inward corner. Significant localized deformations are seen at the intermediate load level. Finally, a discontinuous displacement field can be seen indicating fully developed cracks at the highest load level. The location of the crack seen in Fig. 6 and illustrated in Fig. 10 matches well where displacement gradient (strain) in Fig. 11 is large.

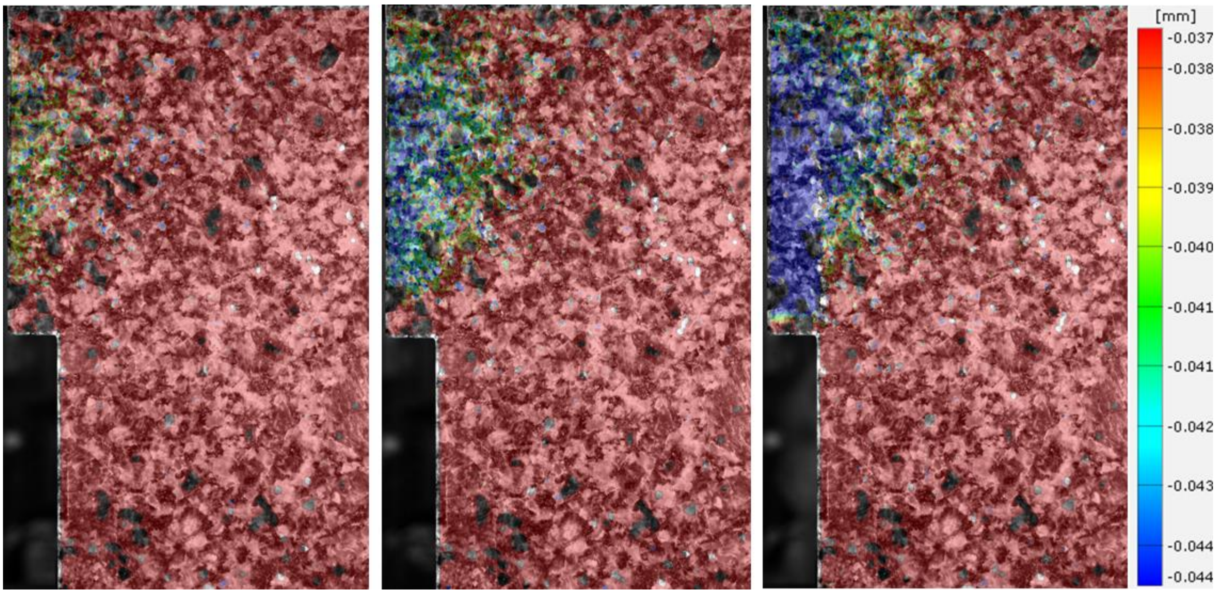

Fig. 11 Lateral displacements (x-direction) for part of the specimen C2 at three loading stages, F = {111.7, 120.4, 126.8} kN.

4 Discussion and conclusion

Looking closer to the crack propagation process, there is an interplay between the stress state and the actual microstructure. This results in a variation in the results between the three specimen geometries. The results of the experiments show that parallel cracks form in some cases when the specimens are loaded. That is when cracks seem to enter grains which are difficult for the cracks to penetrate, and new crack paths are found. The results from the acoustic emission monitoring match well with the preliminary observation and assessment of crack events from the images taken from the specimens. Further analysis of the results will be undertaken at a later stage. Finally, the shear stress is largest at the inward corner, whereas the crack initiation takes place inside the specimen (away from the corner) where the tensile stress is larger. This supports previous hypothesis and evidence that tensile cracking, mode I, is the fundamental fracture mode in rock.

To use this type of specimen gives a new way to study tensile cracking under a mixed tensile and shear stress state with a somewhat controlled crack propagation rate, that normally would be fast. Moreover, the planar surfaces make it possible to monitor the crack propagation during the loading process. The assessment using acoustic emission monitoring, digital image correlation and the images on the specimens were found to be useful. Future studies would involve numerical modelling of the experiments.

References

Germanovich LN, Dyskin AV (2000) Fracture mechanisms and instability of openings in compression, Int. J Rock Mech. Min. Sci. 37(1-2):263-284. DOI 10.1016/S1365-1609(99)00105-7

Horii H, Nemat-Nasser S (1986) Brittle failure in compression: splitting faulting and brittle-ductile transition. Philosophical Transactions of the Royal Society of London. Series A, Mathematical and Physical Sciences, 319: 337-374: DOI 10.1098/rsta.1986.0101

Jacobsson L, Lindqvist JE (2018) Laboratory investigation of crack initiation on hourglass-shaped granite specimens. EUROCK 2018, Saint Petersburg, Russia, 22-26 May 2018.

Nadan BJ, Engelder T (2009) Microcracks in New England granitoids: A record of thermoelastic relaxation during exhumation of intracontinental crust. GSA Bulletin; 121 (1-2): 80–99. DOI:10.1130/B26202.1